J. Am. Chem. Soc. 1992, 114, 682–688

Sensitizer–Substrate Interactions in the 9,10-Dicyanoanthracene-Sensitized Photooxygenation of *trans*-Stilbene

Richard C. Kanner and Christopher S. Foote*

Contribution from the Department of Chemistry and Biochemistry, University of California, Los Angeles, California 90024.

Received April 1, 1991.
Revised Manuscript Received September 6, 1991

Abstract: The quantum yield of singlet oxygen ($^1O_2$) production from 9,10-dicyanoanthracene (DCA) in the presence of *trans*-stilbene (TS) was determined by measurement of its 1268-nm emission. The formation of $^1O_2$ is quenched by TS in acetonitrile but enhanced in benzene. Exciplex emission is observed in both solvents. These observations suggest that exciplex formation in benzene leads to enhanced intersystem crossing in DCA, but that ion-pair separation is too rapid to allow this process in acetonitrile.

Introduction

Previous studies indicate that both Type I (electron transfer) and Type II (singlet oxygen) mechanisms are possible for dicyanoanthracene-sensitized photooxygenation reactions.[1-3] The electron-transfer pathway has been shown for the dicyanoanthracene (DCA)/*trans*-stilbene (TS) system,[4,5] whereas the $^1O_2$ pathway has been demonstrated for the oxidation of other olefins.[2,6,7]

Spectroscopic evidence has been presented for both mechanisms in the DCA-sensitized photooxygenation of TS. Foote and Spada observed both the *trans*-stilbene radical cation (TS$^{\bullet+}$) and the DCA radical anion (DCA$^{\bullet-}$) by transient absorption spectroscopy.[8] DCA$^{\bullet-}$ has also been observed by ESR.[8,9] The yield of free radical ions in the DCA/TS system was determined by Farid and Lewis[5,10] and by transient conductivity.[11] Direct production of $^1O_2$ by energy transfer from both singlet and triplet DCA has been demonstrated by 1268-nm luminescence (see accompanying paper).[3,12] The mechanisms of DCA-sensitized TS photooxygenation and $^1O_2$ production are shown in Scheme I.

Manring et al. showed that there is an additional mechanism for the production of $^1O_2$ involving interaction of the substrate (S) with singlet cyanoaromatic sensitizers in acetonitrile.[13] This mechanism leads to enhanced intersystem crossing for DCA and 9-cyanoanthracene (CA) in acetonitrile, probably via an exciplex, leading to increased triplet production. Heavy-atom-containing and electron-rich substrates enhance $^1O_2$ formation by this mechanism with both sensitizers; TS also causes this process with CA but not with DCA in acetonitrile. Santamaria[14] proposed that the principal mechanism for $^1O_2$ production from DCA is not energy transfer but a substrate interaction similar to that shown by Manring et al.,[13] which leads to the [DCA$^{\bullet-}$···S$^{\bullet+}$] radical ion pair. This ion pair can separate, leading to electron-transfer products, or can collapse to yield the triplet exciplex ^{3}[DCA···S] or triplet DCA (^{3}DCA), one of which produces $^1O_2$ as shown in Scheme II.

Scheme I

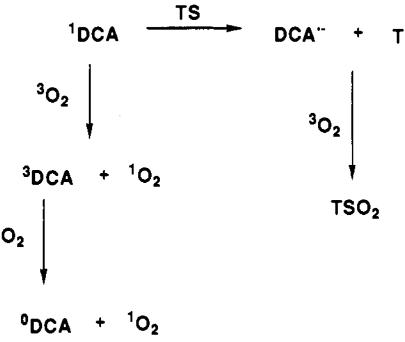

Scheme II

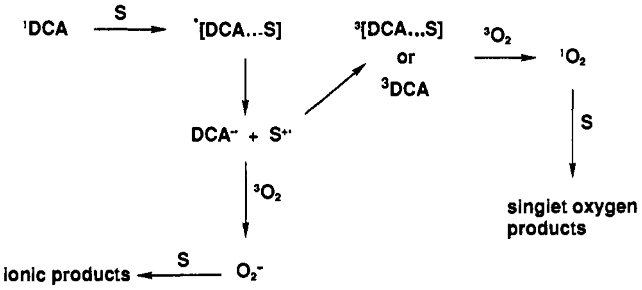

The reaction products of TS have been established for both the electron-transfer and $^1O_2$ pathways and are indicative of the active pathway.[4,5,15] In the $^1O_2$ reaction, the major initial product is the diendoperoxide; however, the rate of reaction of $^1O_2$ with TS is very slow.[3,15] The electron-transfer pathway yields mainly benzaldehyde, with variable amounts of *trans*-stilbene oxide and benzil. In this paper, we use the 1268-nm luminescence of $^1O_2$ as a function of TS in benzene and acetonitrile as a direct probe of some of these steps.

Experimental Section

$^1O_2$ Quantum Yields. The equipment and procedures used are described in the accompanying paper.[3] All samples were irradiated at 355 nm. Singlet oxygen luminescence intensities at time zero were corrected to 100% sensitizer absorbance (from 0.8 at 355 nm) and compared to the

---

(1) Foote, C. S. *Tetrahedron* **1985**, *41*, 2221–2227.

(2) Araki, Y.; Dobrowolski, D. C.; Goyne, T.; Hanson, D. C.; Jiang, Z. Q.; Lee K. J.; Foote, C. S. *J. Am. Chem. Soc.* **1984**, *106*, 4570–4575.

(3) Kanner, R. C.; Foote, C. S. *J. Am. Chem. Soc.*, preceding paper in this issue.

(4) Eriksen, J.; Foote, C. S. *J. Am. Chem. Soc.* **1980**, *102*, 6083–6088.

(5) Lewis, F. D.; Bedell, A. M.; Dykstra, R. E.; Elbert, J. E.; Gould, I. R.; Farid, S. *J. Am. Chem. Soc.* **1990**, *112*, 8055–8064.

(6) Steichen, D. S.; Foote, C. S. *Tetrahedron Lett.* **1979**, 4363–4366.

(7) Cao, Y.; Zhang, B. W.; Ming, Y. F.; Chen, J. X. *J. Photochem.* **1987**, *38*, 131–144.

(8) Spada, L. T.; Foote, C. S. *J. Am. Chem. Soc.* **1980**, *102*, 391–393.

(9) Schaap, A. P.; Zaklika, K. A.; Kaskar, B.; Fung, W.-M. *J. Am. Chem. Soc.* **1980**, *102*, 389–391.

(10) Lewis, F. D.; Dykstra, R. E.; Gould, I. R.; Farid, S. *J. Phys. Chem.* **1988**, *92*, 7042–7043.

(11) Hoyer, W.; Foote, C. S. Manuscript in preparation.

(12) Dobrowolski, D. C.; Ogilby, P. R.; Foote, C. S. *J. Phys. Chem.* **1983**, *87*, 2261–2263.

(13) Manring, L. E.; Gu, C.-L.; Foote, C. S. *J. Phys. Chem.* **1983**, *87*, 40–44.

(14) Truong, T. B.; Santamaria, J. *J. Chem. Soc., Perkin Trans. 2* **1987**, *20*, 1–5.

(15) Kwon, B. M.; Foote, C. S.; Khan, S. I. *J. Org. Chem.* **1989**, *54*, 3378–3382.

0002-7863/92/1514-682$03.00/0

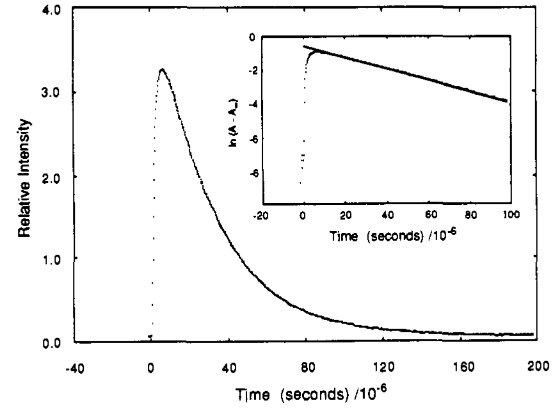

Figure 1. Typical singlet oxygen decay curve sensitized by DCA in air-saturated benzene with no TS, average of 10 laser shots. Inset: Plot of ln ($A - A_\infty$) showing extrapolation to zero time (A = relative intensity).

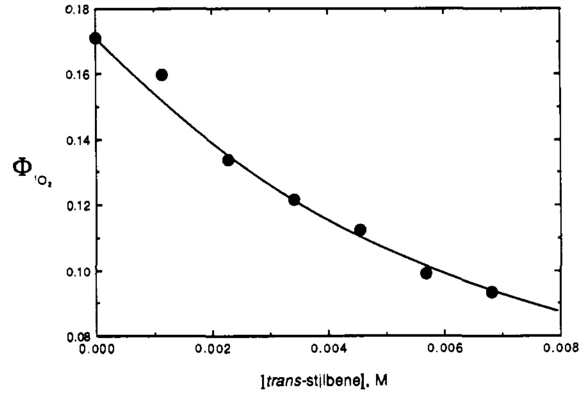

Figure 2. Quantum yield ($\Phi_{^1O_2}$) of $^1O_2$ vs [*trans*-stilbene], sensitized by DCA (1.0×10^{-4} M), irradiated at 355 nm in air-saturated CH_3CN.

$^1O_2$ quantum yield ($\Phi_{^1O_2}$) from DCA in the absence of TS under air, determined by comparison to acridine.[16]

Exciplex Emission. Visible exciplex emission spectra were recorded on a SPEX Fluorolog 2 fluorimeter, exciting DCA (1.2×10^{-7} M) at 355 nm in methylcyclohexane, diethyl ether, benzene, and 1,2-dichloroethane.

Steady-State Near-Infrared Spectra. Near-infrared spectra were taken on a steady-state detection system built by Dr. N. Haegel (UCLA Department of Electrical Engineering), which consisted of a germanium diode (grown in-house) mounted in a liquid-nitrogen-cooled dewar, with a preamplifier operating at room temperature. The output signal was fed into a lock-in amplifier, digitized, and collected on an IBM PC. Wavelength selection was performed with a $^1/_4$-m monochromator (PTI) with a computer-controlled stepper motor (2000-μm slits). Second-order spectra were removed by appropriate cutoff filters. Excitation was carried out with a 300-W Xe lamp (Varian Associates).

Triplet Yields. The equipment and procedures used are described in the accompanying paper.[3] Samples were irradiated at 355 nm in benzene and deaerated by purging with argon for 10 min. ^{3}Acridine, monitored at 440 nm, was used as a standard[17] and compared to the absorbance of ^{3}DCA,[18] monitored at 440 nm as a function of increasing TS concentration.

Materials. DCA (Aldrich Chemical Co.) was recrystallized from toluene. TS (Aldrich) was recrystallized from ethanol. Methylcyclohexene (Aldrich) was used as received. Acridine (Aldrich) was recrystallized from toluene. All solvents were spectroscopic grade (Mallinkrodt) or Gold Label (Aldrich). Deuterated solvents were from Cambridge Isotopes.

Results

A. $^1O_2$ Quantum Yields as a Function of TS. A typical $^1O_2$ decay curve, DCA-sensitized and obtained from the time-resolved luminescence apparatus (TRL), is shown in Figure 1. The inset of Figure 1 shows the fitted line extrapolated back to zero time, giving the initial intensity at the onset of the decay, which is proportional to the $^1O_2$ quantum yield ($\Phi_{^1O_2}$) (see the Experimental Section).

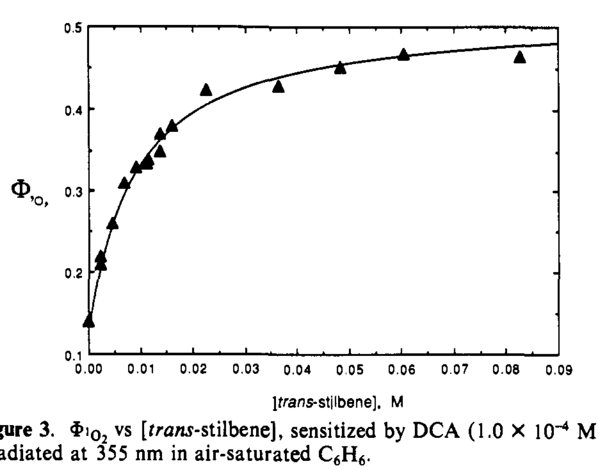

Figure 3. $\Phi_{^1O_2}$ vs [*trans*-stilbene], sensitized by DCA (1.0×10^{-4} M), irradiated at 355 nm in air-saturated C_6H_6.

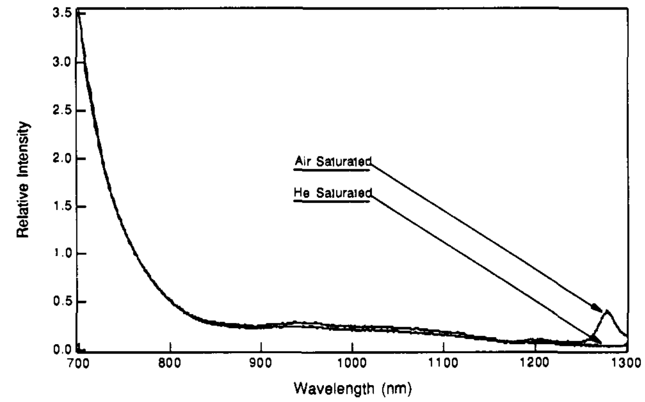

Figure 4. Near-infrared emission from DCA (1.0×10^{-4} M) in acetonitrile in air- and helium-purged solutions.

The $^1O_2$ quantum yield ($\Phi_{^1O_2}$) was measured in this way as a function of [TS] in both acetonitrile and benzene. In CH_3CN, $\Phi_{^1O_2}$ decreases sharply with increasing [TS] (Figure 2). In contrast, $\Phi_{^1O_2}$ increases dramatically with increasing [TS] in benzene (Figure 3).

B. $^1O_2$ Quenching by TS. In the measurement of $\Phi_{^1O_2}$, $^1O_2$ lifetimes decreased appreciably at high TS concentrations in CH_3CN. However, $^1O_2$ formed by rose bengal sensitization was not quenched by TS in CD_3CN at the highest concentrations used. Solubility limited the concentration of TS, so that an exact quenching rate could not be determined. However, the amount of quenching by TS in CH_3CN must be even less than in CD_3CN, in which $^1O_2$ has a much longer lifetime, and therefore cannot be the cause of the decreased lifetime. The quenching rate constant in benzene-d_6 is only 1.15×10^4 M^{-1} s^{-1}, too small to cause appreciable quenching at the concentrations used.

C. Near-Infrared Emission Spectrum. During the course of measuring $\Phi_{^1O_2}$ as a function of [TS], an initial spike in the time-resolved luminescence was observed with a decay <500 ns (resolution of the Ge diode system). This spike increased in intensity with increasing TS concentration. Steady-state near-infrared emission spectra of the DCA/TS system were taken to determine the spectral characteristics of these emissions. Figure 4 shows spectra in CH_3CN from 700 to 1300 nm in the presence and absence of oxygen. The $^1O_2$ peak appears at 1270 nm and is removed when the solution is flushed with He. The large tail beginning at 700 nm is caused by DCA fluorescence, which shows a gradual tail from its maximum at 425 to 850 nm. There is an additional small broad maximum from 900 to 1150 nm, of unknown origin.

Figure 5 shows the emission on addition of TS to the solution under air and with helium purging, and from DCA alone under air. The 1270-nm band of $^1O_2$ is again present with DCA alone but is quenched by TS. In addition, the absence of the hump

---

[16] Redmond, R. W.; Braslavsky, S. E. *Chem. Phys. Lett.* **1988**, *148*, 523–529.

[17] Carmichael, I.; Hug, G. L. *J. Phys. Chem. Ref. Data* **1986**, *15*, 1–250.

[18] Darmanyan, A. P. *Chem. Phys. Lett.* **1984**, *110*, 89–94.

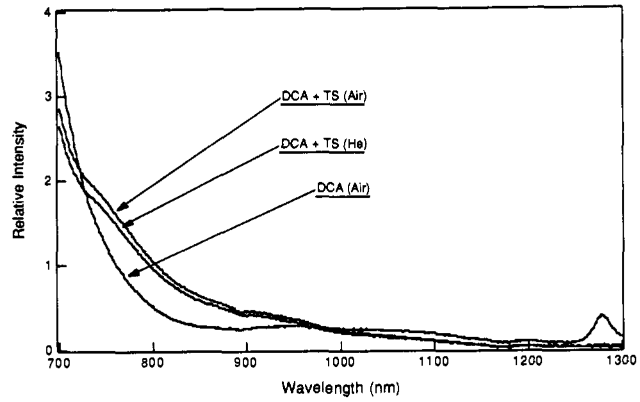

Figure 5. Near-infrared emission of DCA (1.0 × 10^{-4} M) alone and with added TS (2.46 × 10^{-4} M) in acetonitrile in air- and helium-purged solutions. DCA was excited at 400 nm.

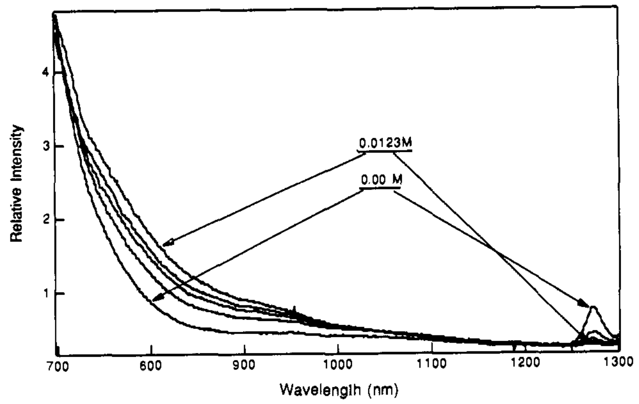

Figure 6. Concentration dependence of emission intensity in CH_3CN on [TS] at 0.00, 0.001 23, 0.002 46, 0.003 69, and 0.0123 M. DCA (1.0 × 10^{-4} M) was excited at 400 nm.

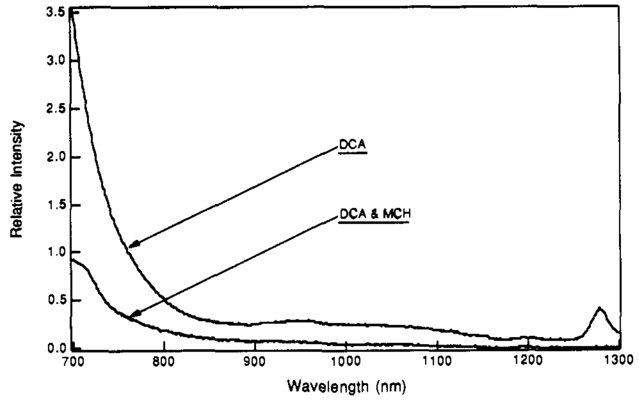

Figure 7. Emission of DCA (1.0 × 10^{-4} M) with and without methylcyclohexene (MCH, 0.169 M) in CH_3CN and air.

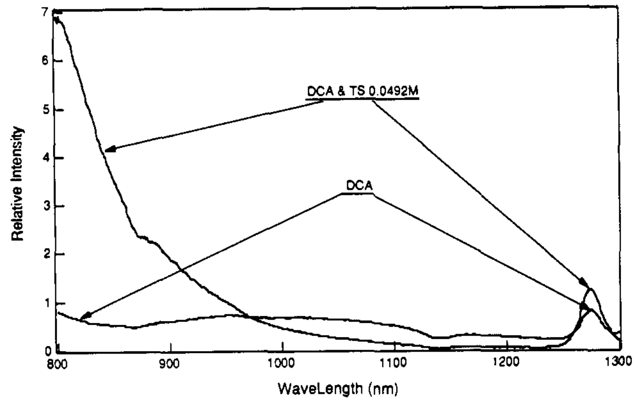

Figure 8. Near-infrared emission spectrum of DCA (2.6 × 10^{-4} M) with and without TS (0.0492 M) in benzene. DCA was excited at 400 nm.

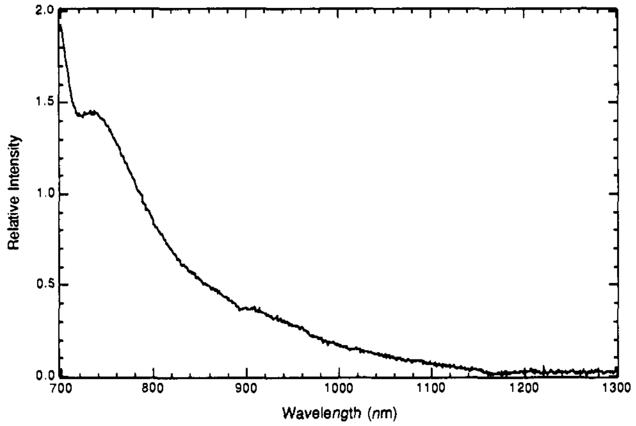

Figure 9. Difference spectrum of DCA with TS (3.46 × 10^{-2} M TS) and MCH (0.169 M).

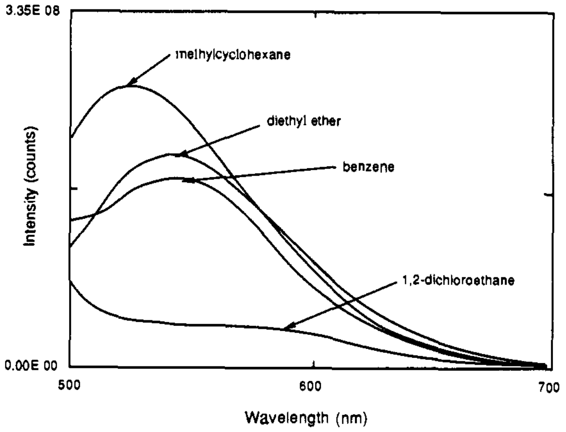

Figure 10. Exciplex emission of DCA/TS in benzene, diethyl ether, 1,2-dichloroethane, and methylcyclohexane. DCA (1.0 × 10^{-6} M) and TS (0.1 M) were excited at 355 nm.

between 900 and 1150 nm and the quenching of the fluorescence of DCA near 700 nm are indicative of ^{1}DCA quenching by TS.

However, Figure 5 also shows that there is an increased emission associated with TS between 750 and 950 nm that appears to be oxygen-independent. These results clearly show that the new emission caused by the addition of TS is not oxygen-induced and that TS quenches both the $^1O_2$ emission in CH_3CN and the DCA fluorescence tail at 700 nm. Figure 6 shows that the intensity of the new emission increases with increasing TS. Stilbene alone does not show any substantial emission in this region.

As a comparison, Figure 7 shows the near-IR emissions from DCA and methylcyclohexene (MCH) in acetonitrile. This spectrum shows that MCH simply quenches the fluorescence of DCA without producing any new emission.

Finally, Figure 8 shows corresponding spectra from the DCA/TS system in C_6H_6. In contrast to the results in CH_3CN, when TS is added the 1270-nm emission of $^1O_2$ *increases*, consistent with the results of the time-resolved experiments. In addition, exciplex emission is observed beginning at 540 nm and tailing to 800 nm (visible data not shown). The weak DCA emission between 900 and 1150 nm seen in CH_3CN is also present in C_6H_6 and is again quenched by TS. No other emissions were found beyond 1500 nm, although the PbS detector used for the long-wavelength search was less sensitive than the germanium diode by about 2 orders of magnitude.

It is likely that the weak infrared emission results from the exciplex formed between excited DCA and TS. The difficulty in determining the wavelength maximum from this data is that the emission, which increases with stilbene concentration, is overlaid on a much stronger fluorescence tail, which is quenched as the stilbene concentration increases. The emission shows a

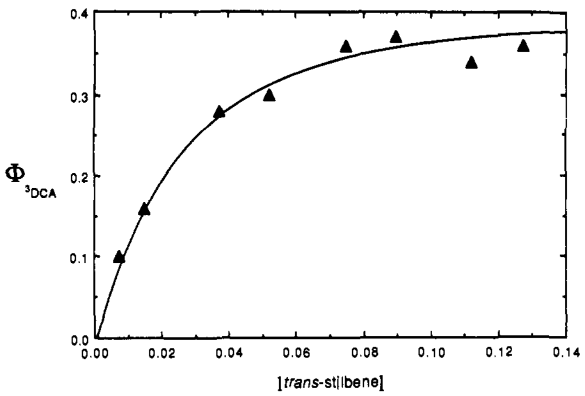

Figure 11. ^{3}DCA quantum yield ($\Phi_{^3DCA}$) versus [*trans*-stilbene] in deoxygenated benzene, 355-nm excitation. ^{3}DCA was monitored at 440 nm (ϵ_{440} = 9000 cm^{-1} M^{-1}).[18] The absorbance of ^{3}DCA was compared to that of ^{3}acridine, with ϵ_{440} = 26 000 cm^{-1} M^{-1} at 440 nm, $\Phi_{^3acridine}$ = 0.84 in benzene.[16,17]

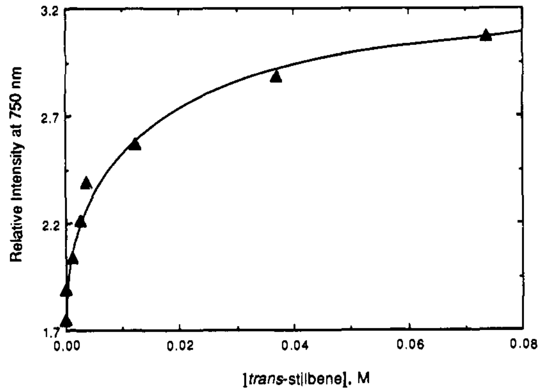

Figure 12. Relative intensity of the emission at 750 nm versus [*trans*-stilbene] in acetonitrile.

shoulder at 725 nm, but is still rising toward shorter wavelengths where our detector loses sensitivity (Figure 9). The true wavelength maximum of this emission was kindly measured by Dr. S. Farid to be 643 nm (data not shown).[19]

D. DCA/TS Exciplex Emission in Various Solvents. Exciplex emission for the DCA/TS system was measured in various solvents, and the results are shown in Figure 10. Our equipment was too insensitive to allow measurement of visible exciplex emission in acetonitrile.[19] The emission maximum in benzene at 537 nm is in reasonable agreement with the value reported by Lewis of 533 nm.[20] The shift toward longer wavelength and decreased intensity with increasing solvent polarity is typical of exciplex emission and very similar to the behavior reported for DCA with cyclohexadiene and dimethoxybenzene.[21]

E. ^{3}DCA Triplet–Triplet Absorption as a Function of TS. In addition to measurement of the $^1O_2$ quantum yield, we also determined the ^{3}DCA yield ($\Phi_{^3DCA}$) in benzene as a function of TS using transient absorption spectroscopy (Figure 11). The absorbance of ^{3}DCA at 440 nm was compared to that of ^{3}acridine to obtain absolute quantum yields (see accompanying paper).[3] Similar measurements were not performed in CH_3CN because the $^1O_2$ quantum yield studies showed that TS decreases the already small yield of ^{3}DCA (0.85% in the absence of oxygen),[3] and previous attempts to measure ^{3}DCA under similar conditions were unsuccessful.[1]

Table I. Emission from TS···^{1}DCA as a Function of Solvent

solvent	$f - {}^1/_2 f'$	ν_{max}, cm^{-1} × 10^{-2}
methylcyclohexane	0.106	191
benzene	0.114	186
diethyl ether	0.256	185
1,2-dichloroethane	0.324	177
acetonitrile	0.393	156[a]

[a] From the measured value of 643 nm by Farid.[19]

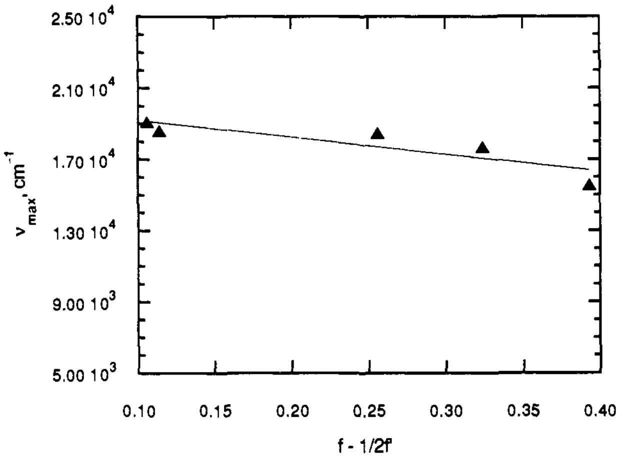

Figure 13. Plot of ν_{max} versus $f - {}^1/_2 f'$ (see eq 1 and Table I) for DCA/TS.

Discussion

DCA/TS Exciplex Emission. The increased emission that occurs on addition of TS to DCA in CH_3CN shown in Figure 5 is probably from the DCA/TS exciplex and, although exciplex emission is extremely weak in solvents this polar, it has been observed on several occasions.[22,23] A plot of the intensity of the luminescence against [TS] (Figure 12) follows saturation kinetics with a concentration dependence suggesting that this luminescence comes from quenching of ^{1}DCA by TS, consistent with the suggestion that it is derived from the singlet exciplex.

A double reciprocal plot of the intensities vs [TS] was attempted (data not shown). Unfortunately this plot showed substantial downward curvature because fluorescence from ^{1}DCA is incompletely corrected by the subtraction procedure at the lower concentrations of TS. However, at the highest TS concentrations, a reasonable linear fit was achieved.

Exciplex emission would be expected to be strongly red-shifted and to have much lower intensity in CH_3CN than in C_6H_6. This effect is described by the Lippert equation:[24]

$$\nu_{max} = \nu_0 \frac{2\mu^2}{hca^3}\left(\frac{\epsilon - 1}{2\epsilon + 1} - \frac{1}{2}\,\frac{n^2 - 1}{2n^2 + 1}\right) = \nu_0 \frac{2\mu^2}{hca^3}(f - {}^1\!/_2 f') \qquad (1)$$

where ν_{max} is the wavenumber of the emission maximum, ν_0 is the hypothetical gas-phase emission frequency, μ is the exciplex dipole moment, h is Planck's constant, c is the velocity of light, a is the charge separation in the exciplex, ϵ is the solvent dielectric constant, and n is the solvent refractive index. Exciplex emission maxima are summarized in Table I and plotted according to eq 1 in Figure 13. Although the data in acetonitrile deviate somewhat from the line, it shows the usual trend toward longer wavelength emission with increasing solvent polarity.

The relative intensities of the exciplex emission at 725 nm and of $^1O_2$ at 1270 nm allow calculation of the approximate lower limit of the quantum yield of exciplex emission in this wavelength region. The radiative quantum yield for $^1O_2$ is about 1 × 10^{-4} in CH_3CN,[25,26] and the quantum yield of $^1O_2$ formation is 0.17 from DCA

---

(19) Farid, S. Private Communication, 1991.

(20) Lewis, F. D.; Dykstra, R. E. *J. Photochem. Photobiol., A: Chemistry* **1989**, *49*, 109–119.

(21) Eriksen, J.; Foote, C. S. *J. Phys. Chem.* **1978**, *82*, 2659–2662.

(22) Kikuchi, K.; Niwa, T.; Takahashi, Y.; Ikeda, H.; Miyashi, T.; Hoshi, M. *Chem. Phys. Lett.* **1990**, *173*, 421–424.

(23) (a) Gould, I. R.; Mueller, L. J.; Farid, S. *Z. Phys. Chem.*, submitted for publication. (b) Gould, I. R.; Moser, J. E.; Ege, O.; Farid, S. *J. Am. Chem. Soc.* **1988**, *92*, 1991–1993.

(24) Lakowicz, J. R. *Principles of Fluorescence Spectroscopy*; Plenum Press: New York, 1984; pp 190–194.

(25) Losev, A. P.; Byteva, I. M.; Gurinovich, G. P. *Chem. Phys. Lett.* **1988**, *143*, 127–129.

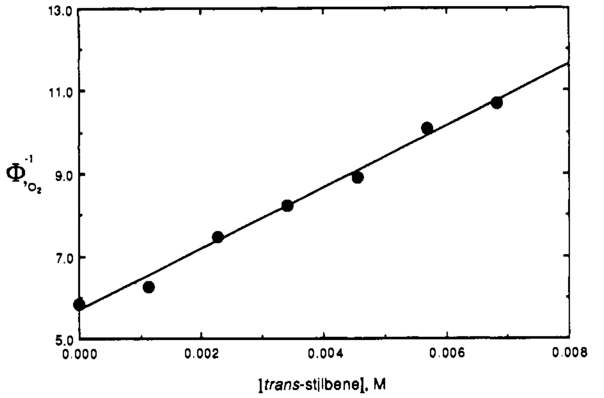

Figure 14. $\Phi^{-1}_{^1O_2}$ versus *trans*-stilbene concentration in CH_3CN.

Scheme III

$$^1\mathrm{DCA} + \mathrm{TS} \xrightarrow{k_{\mathrm{iscts}}} {}^3\mathrm{DCA} + \mathrm{TS}$$

$$^1\mathrm{DCA} + \mathrm{TS} \xrightarrow{k_{\mathrm{qts}}} {}^0\mathrm{DCA} + \mathrm{TS}$$

$$^1\mathrm{DCA} + \mathrm{TS} \xrightarrow{k_{\mathrm{fts}}} {}^0\mathrm{DCA} + \mathrm{TS} + h\nu'' \text{ (exciplex luminescence)}$$

under air.[3] The intensity of the exciplex emission is roughly 10–20 times larger than that of $^1O_2$ (Figure 6). Consequently, the quantum yield of exciplex emission is about 0.04%, corrected to 100% quenching of DCA[1] by TS. This emission does not represent a significant pathway for deactivation of the exciplex but may account for the initial spike in the $^1O_2$ time-resolved spectra if not completely removed by the filters in the laser experiment.

Kinetic Analysis of TS/DCA System in CH_3CN. On the basis of the mechanism outlined below, $^3O_2$ and TS compete for ^{1}DCA, producing either $^1O_2$ or ions, respectively. The processes involved in $^1O_2$ production are outlined in the accompanying paper.[3] Both ^{1}DCA and ^{3}DCA contribute to the production of $^1O_2$.[12]

$$^1O_2 \xleftarrow[{^3O_2}]{} {}^1\mathrm{DCA} \xrightarrow[\mathrm{TS}]{} \mathrm{ions}$$

The additional processes that take place in the presence of TS are listed in Scheme III; TS-induced intersystem crossing of ^{1}DCA is not significant in CH_3CN ($k_{\mathrm{iscts}} = 0$).

$\Phi_{^1O_2}$ is given by eq 2:

$$\Phi_{^1O_2} = \left\{(k_{\mathrm{eto}}{}^1 + k_{\mathrm{sf}}{}^1)[^3O_2] + ((k_{\mathrm{eto}}{}^1 + k_{\mathrm{isco}})[^3O_2] + k_{\mathrm{isc}}) \left(\frac{k_{\mathrm{eto}}{}^3[^3O_2]}{k_{\mathrm{ox}}{}^3[^3O_2] + \tau^{-1}_{^3\mathrm{DCA}}}\right)\right\} / \{k_{\mathrm{ox}}{}^1[^3O_2] + k_q[\mathrm{TS}] + \tau^{-1}_{^1\mathrm{DCA}}\} \quad (2)$$

where lumped constants are defined in the accompanying paper[3] and k_q is the sum of all of the processes for DCA quenching by TS:

$$k_q = k_{\mathrm{qts}} + k_{\mathrm{iscts}} + k_{\mathrm{fts}}$$

Taking the reciprocal of eq 2 yields eq 3,

$$\Phi^{-1}_{^1O_2} = \frac{k_{\mathrm{ox}}{}^1[^3O_2] + \tau^{-1}_{^1\mathrm{DCA}}}{A} + \frac{k_q[\mathrm{TS}]}{A} \quad (3)$$

where A is defined as follows:

$$A = (k_{\mathrm{eto}}{}^1 + k_{\mathrm{sf}}{}^1)[^3O_2] + ((k_{\mathrm{eto}}{}^1 + k_{\mathrm{isco}})[^3O_2] + k_{\mathrm{isc}})\left(\frac{k_{\mathrm{eto}}{}^3[^3O_2]}{k_{\mathrm{ox}}{}^3[^3O_2] + \tau^{-1}_{^3\mathrm{DCA}}}\right) \quad (4)$$

A plot of $\Phi^{-1}_{^1O_2}$ vs TS is shown in Figure 14. The excellent linear dependence is fully consistent with the competitive inhibition by TS of singlet oxygen formation from ^{1}DCA. The data calculated from this plot are summarized in Table II.

Kinetic Analysis in C_6H_6. In contrast to the situation in CH_3CN, addition of TS in C_6H_6 causes $^1O_2$ production from DCA to increase. Scheme IV outlines a mechanism for this increase that involves TS-enhanced intersystem crossing. From this mechanism, $\Phi_{^1O_2}$ is as follows:

$$\Phi_{^1O_2} = \frac{k_{\mathrm{eto}}{}^1[^3O_2]}{k_{\mathrm{ox}}{}^1[^3O_2] + k_q[\mathrm{TS}] + \tau^{-1}_{^1\mathrm{DCA}}} + \left(\frac{(k_{\mathrm{eto}}{}^1 + k_{\mathrm{isco}})[^3O_2] + k_{\mathrm{isc}} + k_{\mathrm{iscts}}[\mathrm{TS}]}{k_{\mathrm{ox}}{}^1[^3O_2] + k_q[\mathrm{TS}] + \tau^{-1}_{^1\mathrm{DCA}}}\right) S_\Delta \quad (5)$$

where S_Δ was previously defined in the accompanying paper.[3] As derived in the accompanying paper, the singlet oxygen quantum yield is the following:

$$\Phi_{^1O_2} \times F = C + S_\Delta k_{\mathrm{iscts}}[\mathrm{TS}] \quad (6)$$

F, the total rate of decay of ^{1}DCA in the presence of quenchers, can be calculated from the data in the accompanying paper and the quenching rate constants of ^{1}DCA by TS: 9.60 × 10^9 in C_6H_6[27] and 1.88 × 10^{10} in CH_3CN.[21] Figure 15 is a plot of the data according to eq 6; data calculated from this plot are summarized in Table II.

From Figure 15, it is clear that the data are well fit by the kinetic expressions derived, with the assumption that ^{3}DCA formed by enhanced intersystem crossing is the source of $^1O_2$. As expected, the lower energy triplet is produced (^{3}DCA ≈ 41.8 kcal/mol, rather than ^{3}TS, 49 kcal/mol).[28] In any case, ^{3}TS could not be the source of $^1O_2$ since its S_Δ value is only 0.18[29] and $\Phi_{^1O_2}$ reaches 0.4 at high TS concentrations (Figure 2).

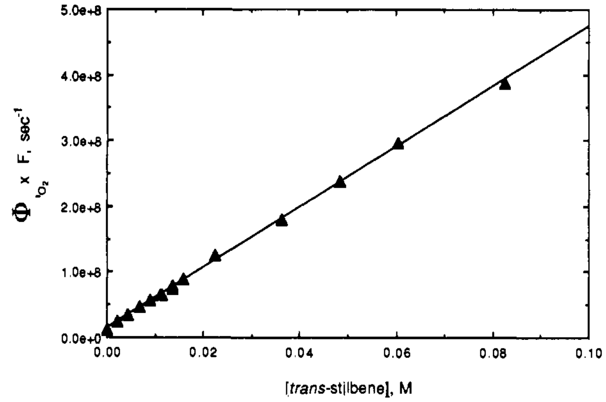

Figure 15. $\Phi_{^1O_2} \times F$ versus *trans*-stilbene in C_6H_6.

Table II. Kinetic Parameters Derived from Plots of Various Equations

eq	param	slope	param	intercept	corr coeff
3	k_q/A	7.44 × 10^2, M^{-1}	$(k_{\mathrm{ox}}{}^1[^3O_2] + \tau^{-1}_{^1\mathrm{DCA}})/A$	5.68	0.991
6	$S_\Delta k_{\mathrm{iscts}}$	4.58 × 10^9, s^{-1}	C	6.5 × 10^9	0.999
7	$\tau^{-1}_{^1\mathrm{DCH}}/k_{\mathrm{iscts}}$	5.96 × 10^{-2}, M	k_q/k_{iscts}	2.07	0.998

Scheme IV

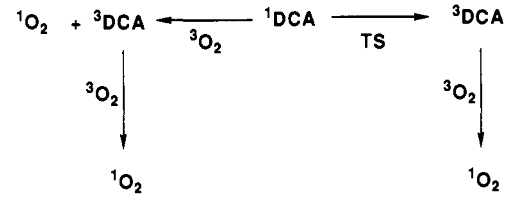

---

(26) Scurlock, R. D.; Ogilby, P. R. *J. Phys. Chem.* **1987**, *91*, 4599–4602.

(27) Eriksen, J.; Foote, C. S. Unpublished Observation.

(28) Birks, J. B. *Photophysics of Aromatic Molecules*; Wiley-Interscience: New York, 1970.

(29) Gorman, A. A.; Rodgers, M. A. J. *Chem. Phys. Lett.* **1985**, *120*, 58–62.

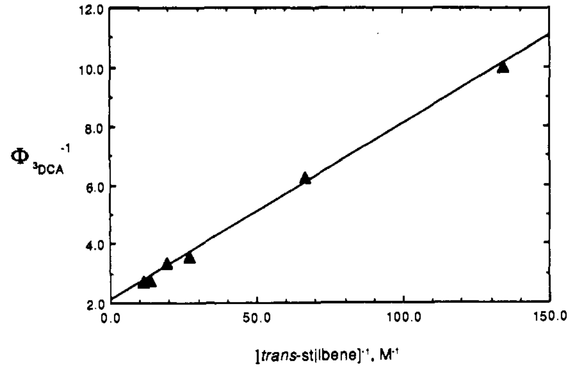

Figure 16. Plot of the triplet quantum yield data according to eq 7.

^{3}DCA Yields from TS. From Scheme IV, $\Phi^{-1}_{^3\mathrm{DCA}}$ is given by eq 7.

$$\Phi^{-1}_{^3\mathrm{DCA}} = \frac{k_q}{k_{\mathrm{iscts}}} + \frac{\tau^{-1}_{^1\mathrm{DCA}}}{k_{\mathrm{iscts}}[\mathrm{TS}]} \tag{7}$$

A plot of the triplet quantum yield data according to eq 7 is shown in Figure 16. When [TS] = ∞, eq 7 reduces to

$$1/\Phi_{^3\mathrm{DCA}} = k_q/k_{\mathrm{iscts}}$$

From Figure 16, $\Phi_{^3\mathrm{DCA}}$ at [TS] = ∞ is 48%, and the resulting value of k_{iscts} is 4.6 × 10^9 M^{-1} s^{-1}. Alternatively, k_{iscts} can be calculated from the value of $S_\Delta k_{\mathrm{iscts}}$ obtained from the $^1O_2$ quantum yield measurements (Table II). S_Δ is 70% (see accompanying paper), giving a value of k_{iscts} = 6.5 × 10^9 M^{-1} s^{-1}, which would give a calculated value for $\Phi_{^3\mathrm{DCA}}$ of 67% at [TS] = ∞. These numbers are in reasonable agreement, considering the errors, and show that TS induces intersystem crossing in DCA with high efficiency in benzene.

Quenching of $^1O_2$. We noted up to a 35% decrease in $^1O_2$ lifetime at the highest concentration of TS in CH_3CN. However, as discussed in the Results section, the rate of $^1O_2$ quenching in CH_3CN is far too slow to account for this. Consequently, the $^1O_2$ lifetime change must be caused by something else. Quenching by superoxide ($O_2^{\bullet-}$), which has a rate constant of 1.6 × 10^9 M^{-1} s^{-1},[30] would provide a possible explanation for the lifetime shortening, which is not observed in C_6H_6 where free ions are not formed.

Mechanism. This study has revealed some interesting aspects of the mechanism of DCA-sensitized photooxygenation of TS. In CH_3CN, the mechanism is clearly electron transfer or Type I, with $^1O_2$ being produced only at low concentrations of TS, as suggested in previous reports.[4,8,31,32] In C_6H_6, the mechanism is purely $^1O_2$ or Type II, which is also consistent with previous reports.[2,7] However, the dramatic increase in $^1O_2$ production at high concentrations of TS and the enhancement of intersystem crossing of ^{1}DCA by TS have not been previously demonstrated.

Similar enhanced intersystem crossing has been shown by Darmanyan for 9,10-dibromo-, -dichloro-, and -dicyanoanthracene singlets quenched by naphthalene, pyrene, fluorene, and biphenyl.[18] Darmanyan suggests that these substituted anthracenes are quenched by charge-transfer interactions, leading to the formation of a short-lived singlet exciplex $^1(A^{\delta-}\cdots D^{\delta+})^*$. The charge-transfer mechanism is reflected by an increase in the ^{1}DCA quenching rate constant, k_q, with increasing solvent polarity (1.88 × 10^{10} in CH_3CN vs 9.6 × 10^9 in C_6H_6). A recent paper by Takahashi et al.[33] has shown that 1,4-diphenyl-1,3-butadiene also enhances the intersystem crossing of DCA in CCl_4.

In general, the formation of an exciplex is the first step in the quenching of excited states, followed by electron transfer and ion separation in polar solvents. Although a recent paper by Gould et al.[34] suggested that electron transfer between a free donor and acceptor can occur while the donor and acceptor are solvent-separated in polar solvents, this was not observed in quenching of ^{1}DCA by any of the donors studied. In addition, the calculated value of the exciplex energy of 61.6 kcal/mol (calculated from the emission maximum at 643 nm and a reorganization energy of 17.2 kcal/mol)[34] is above that of the separated ions (calculated from redox potentials to be 56.4 kcal/mol in CH_3CN), suggesting that exciplex formation is a precursor of the separated ions. Assuming that electron transfer is the first step in the deactivation of ^{1}DCA, that the triplet is formed from a triplet exciplex,[18] and that emission is from the singlet exciplex, we propose the mechanism in Scheme V on the basis of the pioneering analysis of Gould, Farid, et al.[23,34,35]

Scheme V

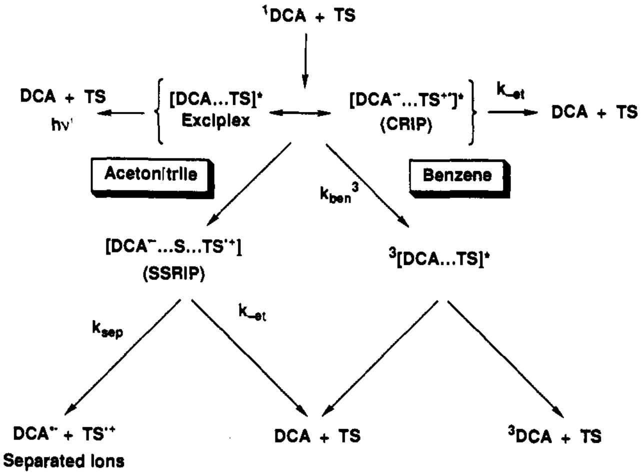

Initially, ^{1}DCA is quenched to form a hybrid of a locally excited exciplex (DCA*$\cdots$TS) and a contact radical ion pair (CRIP) (DCA$^{\bullet-}\cdots$TS$^{\bullet+}$). Gould et al. suggest that this hybrid is almost exclusively CRIP in acetonitrile in very similar cases.[34] The CRIP can either give back-electron-transfer (k_{-et}) or decay to a ground-state complex.[23,34,35] In CH_3CN, solvation of the CRIP is rapid and leads to a solvent-separated radical ion pair (SSRIP), which can either give back-electron-transfer (k_{-et}) or separate (k_{sep}) to form free ions. Back-transfer is relatively slow since this ion pair is in the Marcus inverted region,[5,10,20] and dissociation is rapid. The consequence is that the exciplex lifetime is very short, and its emission is consequently very weak; there is a relatively high yield of free ions. We assume that only a singlet exciplex is formed, since no ^{3}DCA is observed in CH_3CN in the presence of TS.[1] In addition, the yield of ^{3}DCA from this path cannot be significant because the plot of $^1O_2$ quantum yields vs TS in CH_3CN is fit well with no assumption of enhanced intersystem crossing.

In C_6H_6 by contrast, there is no dissociation because of the low solvent polarity, and the exciplex is relatively long lived and has time to emit or to undergo intersystem crossing to form the triplet exciplex in competition with back-electron-transfer. The overall route to ^{3}DCA has a 40% efficiency (Table II). The singlet exciplex can either emit or decay nonradiatively.

The mechanism of enhanced $^1O_2$ production in nonpolar solvents described here is similar to that proposed by Santamaria.[14] However, Santamaria's mechanism does not include the formation of $^1O_2$ from DCA in the absence of substrate. Furthermore, in the photooxygenation of 1,4-dimethylnaphthalene (DMN) in polar solvents,[14,36] ^{3}DCA is suggested to be produced from the radical ion pair, which in turn yields $^1O_2$ (see Scheme IV). The results

---

(30) Guiraud, H. J.; Foote, C. S. *J. Am. Chem. Soc.* **1976**, *98*, 1984–1986.

(31) Steichen, D. S.; Foote, C. S. *J. Am. Chem. Soc.* **1981**, *103*, 1855–1857.

(32) Manring, L. E.; Eriksen, J.; Foote, C. S. *J. Am. Chem. Soc.* **1980**, *102*, 4275–4277.

(33) Takahashi, Y.; Wakamatsu, K.; Kikuchi, K.; Miyashi, T. *J. Phys. Org. Chem.* **1990**, *3*, 509–518.

(34) Gould, I. R.; Young, R. H.; Moody, R. E.; Farid, S. *J. Phys. Chem.* **1991**, *95*, 2068–2080.

(35) Gould, I. R.; Young, R. H.; Farid, S. In *Photochemical Processes in Organized Molecular Systems*; Elsevier: Amsterdam, 1991.

(36) Bokobza, L.; Santamaria, J. *J. Chem. Soc., Perkin Trans. 2* **1985**, 269–271.

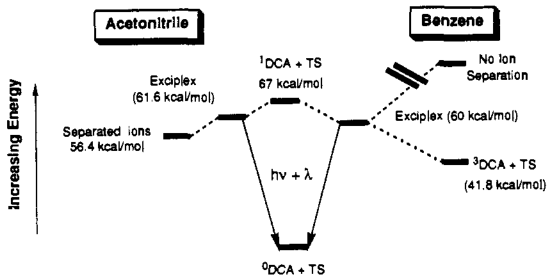

Figure 17. Relative energy diagram of emission and ion separation in CH_3CN and C_6H_6.

of this paper and the accompanying one demonstrate that oxygen directly quenches ^{1}DCA to produce $^1O_2$ in direct competition with other quenchers of ^{1}DCA. DMN quenches ^{1}DCA with a rate constant of 2.54×10^{10} s^{-1} in acetonitrile.[36] Under oxygen saturation ($\sim 10^{-2}$ M) and low ($\sim 10^{-3}$ M) DMN concentrations, oxygen can effectively compete for ^{1}DCA, and $^1O_2$ is produced with 146% efficiency (see the accompanying paper) from each interaction. The energy-transfer pathway to $^1O_2$ is probably dominant under Santamaria's reaction conditions.

Our mechanism can be summarized qualitatively in terms of the relative energy diagram shown in Figure 17. In benzene, the exciplex energy, obtained from the emission spectrum and reorganization energy of 0.3 eV,[19,37] is higher than that of the triplet, but ion-pair separation requires much higher energy, ruling out that pathway completely. Formation of ^{3}DCA competes with singlet exciplex emission. By contrast, in CH_3CN the exciplex (mainly CRIP[34]) has an energy above or near[34] the separated ions, whose relative energies are obtained from their redox potentials.[5,20,21] In Figure 17 we use λ_{max} of the exciplex emission to estimate the energy. However, in a closely related case, Gould et al.[34] report that the CRIP and separated ions have nearly the same energies. The polar solvent favors rapid ion separation and nearly, but not quite completely, suppresses exciplex formation and emission.

Summary

The results of this work show that the time-resolved 1270-nm $^1O_2$ luminescence can be used as an effective probe for the mechanism of photooxygenation reactions. If $\Phi_{^1O_2}$ is affected by substrate, it is necessary to look for substrate–sensitizer interactions and probe the system further. If only the $^1O_2$ lifetime is changed by substrate, a pure $^1O_2$ Type II mechanism is involved. This work also suggests that the production of $^1O_2$ from sensitizers can be subject to dramatic environmental effects and that the yield in homogeneous solution may not be predictive of that in more complex systems. This conclusion is particularly relevant for photodynamic therapy.

Acknowledgment. This work was supported by NSF Grants CHE86-11873 and CHE89-11916 and NIH Grant GM-20081. We thank Prof. N. Haegel (UCLA Dept. of Material Science and Engineering) for the use of spectroscopic equipment, and Dr. Samir Farid (Kodak) for measurement of the acetonitrile exciplex emission maximum and several very helpful discussions.

Registry No. TS, 103-30-0; DCA, 1217-45-4; O_2, 7782-44-7.

---

(37) Gould, I. R.; Ege, D.; Moser, J. E.; Farid, S. *J. Am. Chem. Soc.* **1990**, *112*, 4290-4301.

Electron-Transfer-Induced Valence Isomerization of 2,2′-Distyrylbiphenyl[†]

Arno Böhm,[‡] Klaus Meerholz,[§] Jürgen Heinze,[*,§] and Klaus Müllen[*,‡]

Contribution from the Max-Planck-Institut für Polymerforschung, Ackermannweg 10, D-6500 Mainz, Germany, and Department of Physical Chemistry, University of Freiburg, Albert-Strasse 21, D-7800 Freiburg, Germany. Received May 21, 1991

Abstract: Upon chemical or electrochemical reduction, 2,2′-distyrylbiphenyl (**1**) rearranges into the "bis-benzylic" dianion, 3^{2-}, which can be either protonated to a 9,10-dibenzyl-9,10-dihydrophenanthrene or oxidatively coupled to a cyclobutane species. The mechanism of the electron-transfer-induced skeletal rearrangement is studied by product analysis and by cyclic voltammetry, and the results are compared with the outcome of the photolytic [2 + 2] cycloaddition.

1. Introduction

Over the last few years electron-transfer (ET) induced pericyclic reactions have become increasingly important in the syntheses of polycyclic compounds.[1-5] The increase in reactivity observed when going from the neutral to the corresponding ionic species allows one to bring about skeletal rearrangements for otherwise unreactive or thermolabile substrates.[1,5] In the chemical storage and directed release of solar energy, a key role has been attributed to electron-transfer-induced cycloadditions and valence isomerizations.[6-8]

While a number of publications have pointed out the advantages of an ionic reaction path in Diels–Alder reactions and other thermally allowed cyclization processes,[2,9] the potential of electron-transfer-induced [2 + 2] cycloadditions competing with the

---

[†] Reductive Transformations. 17. Part 16: Alexander, J.; Klabunde, K.-U.; Klärner, F.-G.; Lund, H.; Lund, T.; Müllen, K. *Chem. Ber.*, submitted for publication.

[‡] Max-Planck-Institut.

[§] University of Freiburg.

(1) Bellville, D. J.; Wirth, D. D.; Bauld, N. L. *J. Am. Chem. Soc.* **1981**, *103*, 718. Pabon, R. A.; Bellville, D. J.; Bauld, N. L. *J. Am. Chem. Soc.* **1983**, *105*, 5158. Harirchian, B.; Bauld, N. L. *Tetrahedron Lett.* **1987**, 927.

(2) Fox, M. A.; Hurst, J. R. *J. Am. Chem. Soc.* **1984**, *106*, 7626.

(3) Mlcoch, J.; Steckhan, E. *Tetrahedron Lett.* **1987**, 1081.

(4) Pattenden, G. K.; Robertson, G. M. *Tetrahedron Lett.* **1983**, 4617.

(5) Bauld, N. L.; Bellville, D. J.; Pabon, R.; Chelsky, R.; Green, G. *J. Am. Chem. Soc.* **1983**, *105*, 3584. Bauld, N. L.; Bellville, D. J.; Pabon, R. A.; Chelsky, R.; Green, G. *J. Am. Chem. Soc.* **1983**, *105*, 2378. Bauld, N. L.; Harirchian, B. *J. Am. Chem. Soc.* **1989**, *111*, 1826. Steckhan, E.; et al. *Synlett* **1990**, 275.

(6) Barber, R. A.; de Mayo, P.; Okada, K. *J. Chem. Soc., Chem. Commun.* **1982**, 1073.

(7) Draper, A. M.; de Mayo, P. *Tetrahedron Lett.* **1986**, 6157.

(8) Gassman, P. G.; Hershberger, J. W. *J. Org. Chem.* **1987**, *52*, 1337.

(9) Staley, S. W.; Heyn, A. S. *J. Am. Chem. Soc.* **1975**, *98*, 3852.